CORRECTION OF MIRROR DISTORTION EFFECTS IN BEAM-SIZE MEASUREMENT USING SR INTERFEROMETER

J.W. Flanagan, S. Hiramatsu, H. Ikeda, T. Mitsuhashi, KEK, Tsukuba, Ibaraki, Japan

Abstract

The effective use of the synchrotron radiation interferometer to measure beam sizes depends on the ability to measure and correct for systematic effects introduced by the distortion of the surface of the extraction mirror. At KEKB it has been observed that changing beam currents cause large changes in the apparent beam size due to the heating of the mirror surface. In this paper we discuss methods developed to monitor and correct for this distortion in the operation of the SR interferometer.

1 INTRODUCTION

Beam sizes are measured at KEKB using SR interferometers, one for the 8 GeV High Energy Ring (HER) and one for the 3.5 GeV Low Energy Ring (LER).[1] At either ring, when the beam current increases the temperature of the beryllium extraction mirror rises, causing a deformation of the mirror surface as the mirror block expands. The resulting curvature changes the propagation angles of the light rays which pass the interferometer slits, causing a change in the apparent beam size which can be quite severe (30%).

The situation is illustrated in Figure 1. The heat-deformed mirror surface is shown as a solid black line, as are the light paths from the SR source point to the interferometer slits. The ideal (undeformed) mirror surface and its corresponding light paths are shown as dashed lines. Immediately downstream of the extraction mirror is a dotted line representing a plane where the pinhole mask (discussed below) for measuring mirror distortion is located. The light rays which reach the interferometer slits depart from the source at an angular divergence of θ. The distance between the light rays when they reach the slits (at a distance L from the light source) is D; the corresponding distance at the mask plane (at distance $L\prime$) is $D\prime$. If the distance from the extraction mirror to the mask plane is much smaller than the distance from the source to the mask plane, and for small angular divergences, $\theta \approx D\prime/L\prime$.

If the mirror is undeformed, then $D\prime = D_0\prime$, where $D_0\prime/L\prime = D/L = \theta_0$. Thus, the equation giving beam size σ_{beam} as a function of interference pattern visibility γ, assuming a Gaussian beam, can be expressed as

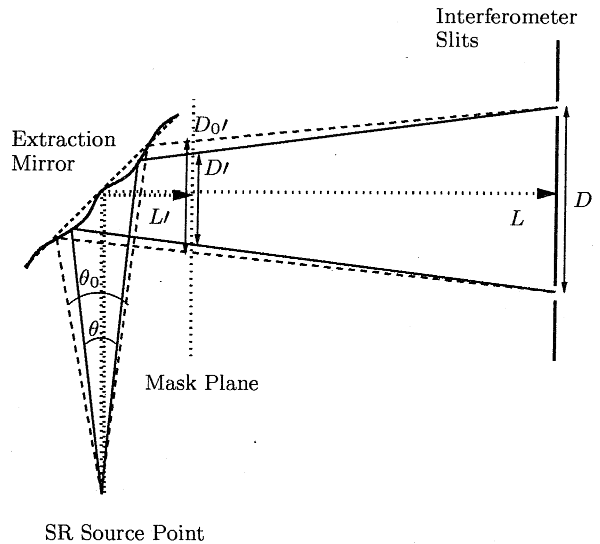

Figure 1: Effect of mirror distortion on ray propagation.

$$\sigma_{beam} = \frac{\lambda}{\pi\theta_0}\sqrt{\frac{1}{2}\ln\frac{1}{\gamma}} = \frac{\lambda L\prime}{\pi D_0\prime}\sqrt{\frac{1}{2}\ln\frac{1}{\gamma}},$$

where λ is the wavelength under observation.

However, in the case of a deformed mirror, $\theta \neq \theta_0$ and $D\prime/L\prime \neq D/L$. In this case, it is necessary to determine $D\prime$ in order to make the correct estimate of the beam size:

$$\sigma_{beam} = \frac{\lambda}{\pi\theta}\sqrt{\frac{1}{2}\ln\frac{1}{\gamma}} = \frac{\lambda L\prime}{\pi D\prime}\sqrt{\frac{1}{2}\ln\frac{1}{\gamma}}. \quad (1)$$

One method of determining $D\prime$ is to use a Hartmann pinhole mask.[2] By moving a pinhole mask across the mask plane, the spots on the mask plane from which light rays propagate to the interferometer slit positions can be easily located (they are the locations at which one or the other slit is illuminated by the SR light which has passed through the pinhole), and $D\prime$ can be measured. $D\prime$ as a function of beam current is shown in Figure 2.

However, this method is not applicable in normal operation, since the interferometer cannot be used when the mask is in place due to one slit being always blocked. For this reason we have developed a method for measuring and correcting for this distortion during real-time operation of the interferometer based on

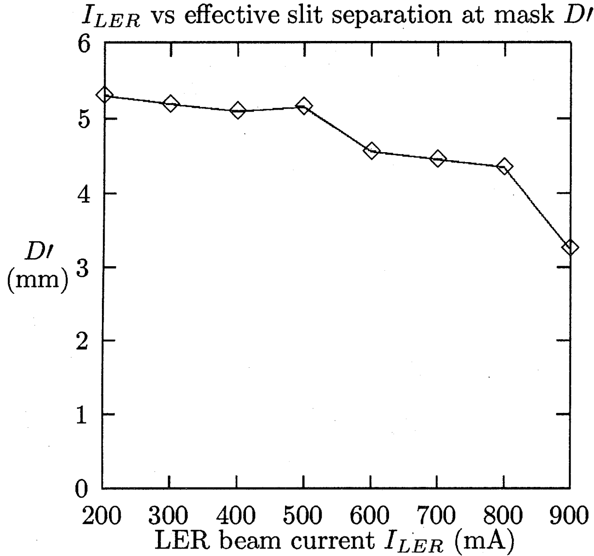

Figure 2: Change in $D\prime$ as a function of beam current due to mirror heating. This corresponds to a change in apparent beam size of $\approx$ 30% as the LER beam current goes from 200 to 900 mA.

modifying the fitting procedure used to analyze the interference pattern visible after the slits.

2 FITTING PROCEDURE

We fit the interference pattern to an equation of the form

$$y(x) = a + bx + \frac{m}{2}\sum_i t_i \times$$
$$\left\{A_1^2 + A_2^2 + 2A_1A_2\gamma^{\left(\frac{\lambda_0}{\lambda_i}\right)^2} \cos\left[\beta_c\left(\frac{\lambda_0}{\lambda_i}\right)(x-\phi_c)\right]\right\},$$

where

$$A_1 = \sqrt{1+\alpha_I}\frac{\sin\left[\beta_s(1+\alpha_s)\left(\frac{\lambda_0}{\lambda_i}\right)\left(x-(\phi_s-\frac{\delta_s}{2})\right)\right]}{\beta_s(1+\alpha_s)\left(\frac{\lambda_0}{\lambda_i}\right)\left(x-(\phi_s-\frac{\delta_s}{2})\right)},$$
$$A_2 = \sqrt{1-\alpha_I}\frac{\sin\left[\beta_s(1-\alpha_s)\left(\frac{\lambda_0}{\lambda_i}\right)\left(x-(\phi_s+\frac{\delta_s}{2})\right)\right]}{\beta_s(1-\alpha_s)\left(\frac{\lambda_0}{\lambda_i}\right)\left(x-(\phi_s+\frac{\delta_s}{2})\right)}.$$

This represents two single-slit diffraction terms of amplitude A_1 and A_2 brought into overlap by the lens behind the slits, modulated by a cosine double-slit term with visibility γ determined by the spatial coherence of the SR light. The cos term has a period determined by β_c, with offset ϕ_c. The resulting pattern is of magnitude m, with a linear background term $a + bx$.

To account for bandpass effects which would otherwise artificially lower the visibility, we write the fitting function as a sum over a sample of wavelengths

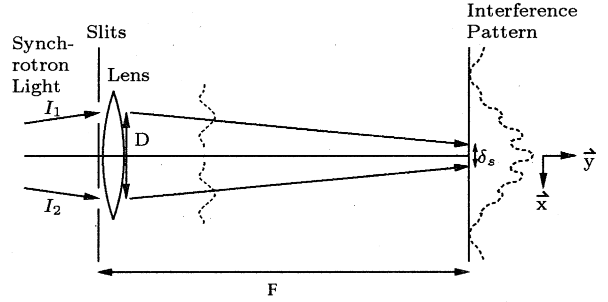

Figure 3: Interference pattern formation.

λ_i passed by the bandpass filter with central frequency λ_0, each term weighted by the transmission t_i at wavelength λ_i. The incident SR spectrum changes by only a few percent over the bandwidth used (10 nm, centered around 500 nm), and is taken as flat. The exponent appearing on γ represents the variation of visibility observed at different wavelengths relative to that observed at the central wavelength, assuming a Gaussian beam with the same apparent beam size at all wavelengths (i.e., using Equation 1).

In A_1 and A_2, α_I represents the asymmetry $\frac{I_1-I_2}{I_1+I_2}$ of the light intensities I_1 and I_2 impinging on the two slits. $\beta_s(1\pm\alpha_s)$ represent the widths of the single-slit *sinc* terms from each slit, with α_s representing the (usually very small) asymmetry between the widths of the patterns from each slit. $\phi_s \pm \frac{\delta_s}{2}$ represent the centers of the single-slit terms, separated by δ_s from each other.

Changes in δ_s are correlated with deformations in the mirror. The reason for this is that as $D\prime$ after the mirror changes, the angle between the rays reaching the slits changes. This in turn causes the angles between the rays after the lens to change. Since the surface of the camera CCD remains at a fixed distance (F) from the slits/lens, the centers of the single-slit terms A_1 and A_2 move relative to each other on the CCD surface. By measuring the change in δ_s the deformation can be monitored and corrected for in real-time during interferometer usage.

The most important feature of the new fitting procedure which directly corrects for the effect of mirror distortion on apparent beam size is the inclusion of the δ_s term. The fit procedure previously used[3] can be derived from the current one by holding δ_s, α_I and α_s at zero. The light intensity asymmetry parameter α_I corrects for the secondary effects of changes in the light distribution due to mirror distortion.

3 CALIBRATION

For small values of δ_s relative to the longitudinal coherence depth, the relationship between $D\prime$ and δ_s should be approximately linear. To measure this, we took calibration data over the full range of beam cur-

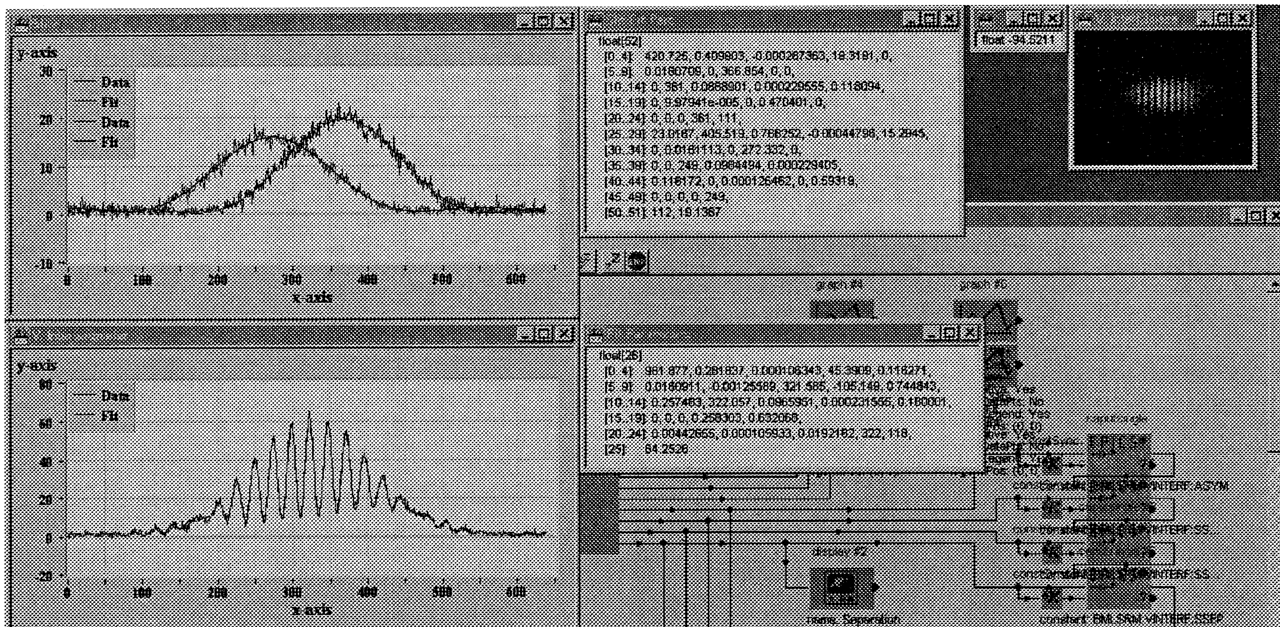

Figure 4: Screenshot of image-processing computer in LER optics hut during image acquisition and analysis.

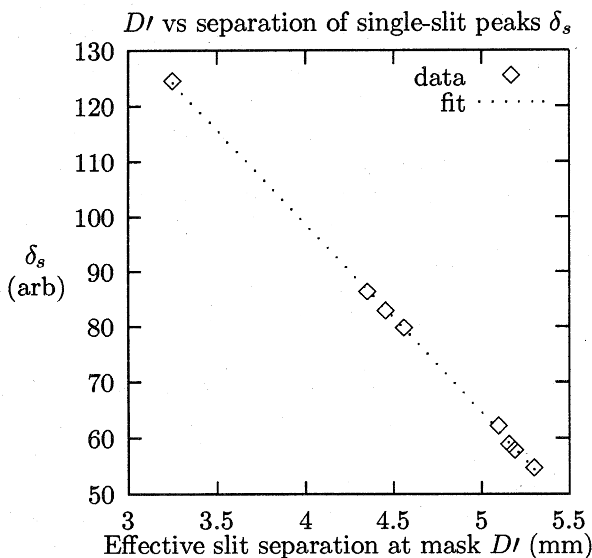

Figure 5: $D\prime$ vs δ_s

rents in use, and plotted the effective slit separation at the mask plane $D\prime$ versus δ_s. The data are shown in Figure 5. The standard deviation to a linear fit is less than one percent, verifying that δ_s can be used to estimate $D\prime$ without needing to use the pinhole mask after initial calibration.

4 OPERATION

Figure 4 shows the screen of the image processing computer in the optics hut. In the upper left graph are shown the single-slit components, measured with a remote-controlled shutter which can be used to block the light from one slit at a time. Below that is the double-slit pattern, fit using the width of the single-slit patterns as measured from the shutter data. Preliminary tests of the system in the Spring of 2001 at the KEKB LER indicate that the method works well.

It should be noted that another approach to this problem would be to put the slits in the tunnel just after the extraction mirror. This would greatly reduce the magnification changes. However, because the angle of incidence on the slits/lens determines the separation of the single-slit terms on the camera CCD plane, it would still be necessary to take δ_s into account in order to make accurate fits.

5 ACKNOWLEDGMENTS

The authors wish to thank Professors S. Kurokawa and K. Oide for their encouragement of this work. The authors also thank the KEKB commissioning team for their support and feedback.

6 REFERENCES

[1] T. Mitsuhashi, J.W. Flanagan, S. Hiramatsu, "Optical Diagnostic System for the KEK B-Factory," Proceedings of EPAC 2000, Vienna, Austria, p. 1783

[2] D. Malacara, ed., Optical Shop Testing, Second edition, Wiley (New York) 1992, pp. 367-396.

[3] J.W. Flanagan, S. Hiramatsu, T. Mitsuhashi, "Automatic Continuous Transverse Beam-size Measurement System for KEKB," Proceedings of EPAC 2000, Vienna, Austria, p. 1714